Neuron, Volume 64

Supplemental Data

Molecular Identification of Rapidly Adapting Mechanoreceptors and Their Developmental Dependence on Ret Signaling

Wenqin Luo, Hideki Enomoto, Frank L. Rice, Jeffrey Milbrandt, and David D. Ginty

Supplemental Figures

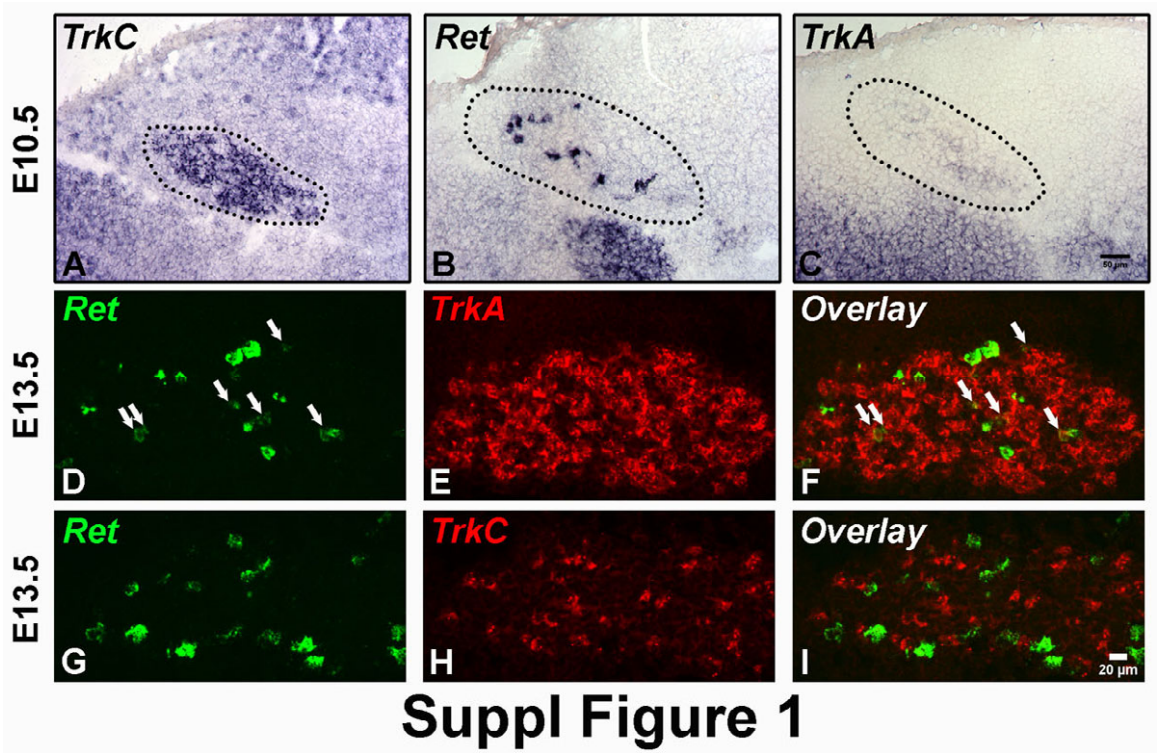

Suppl Figure 1

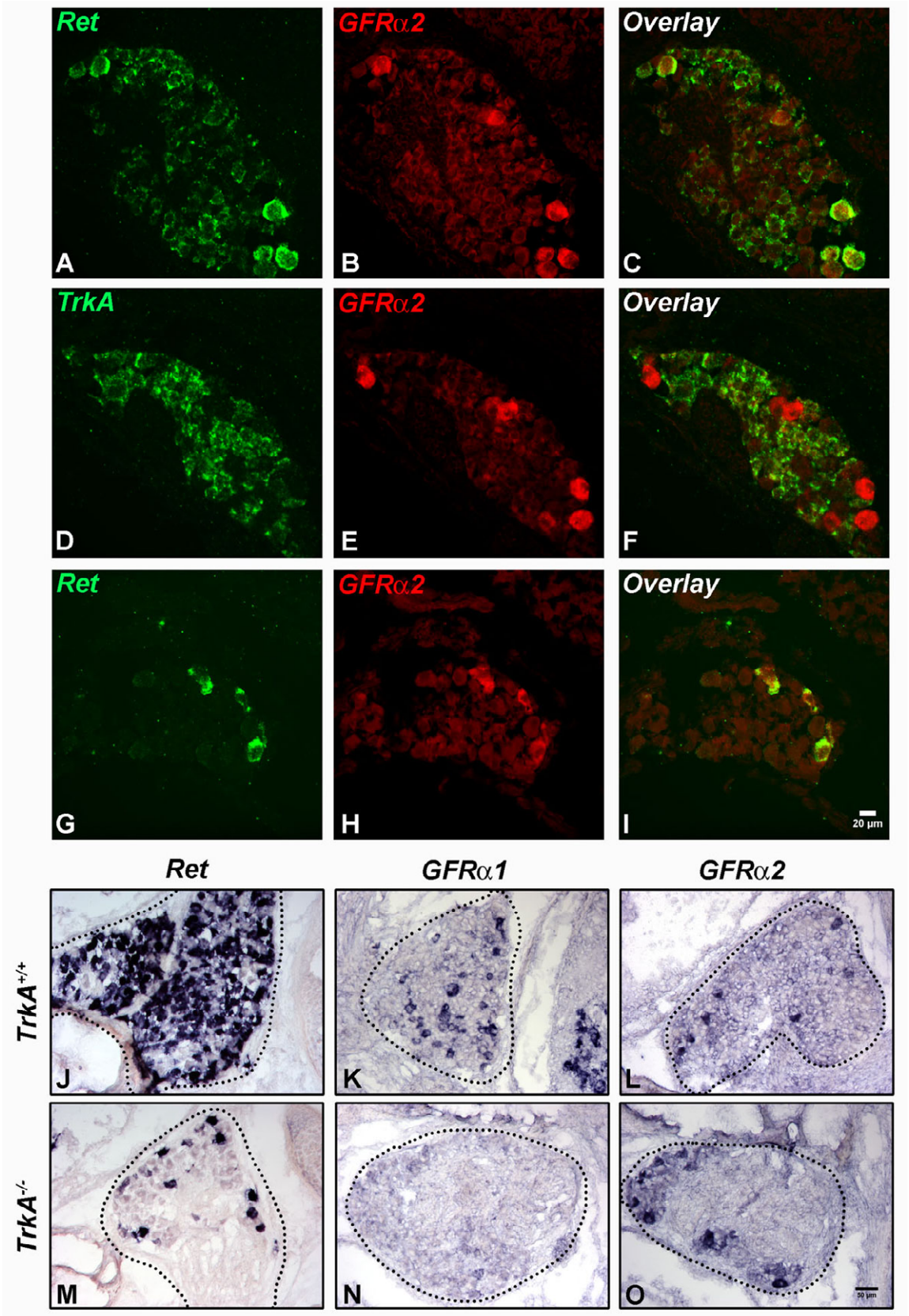

Suppl Figure 2

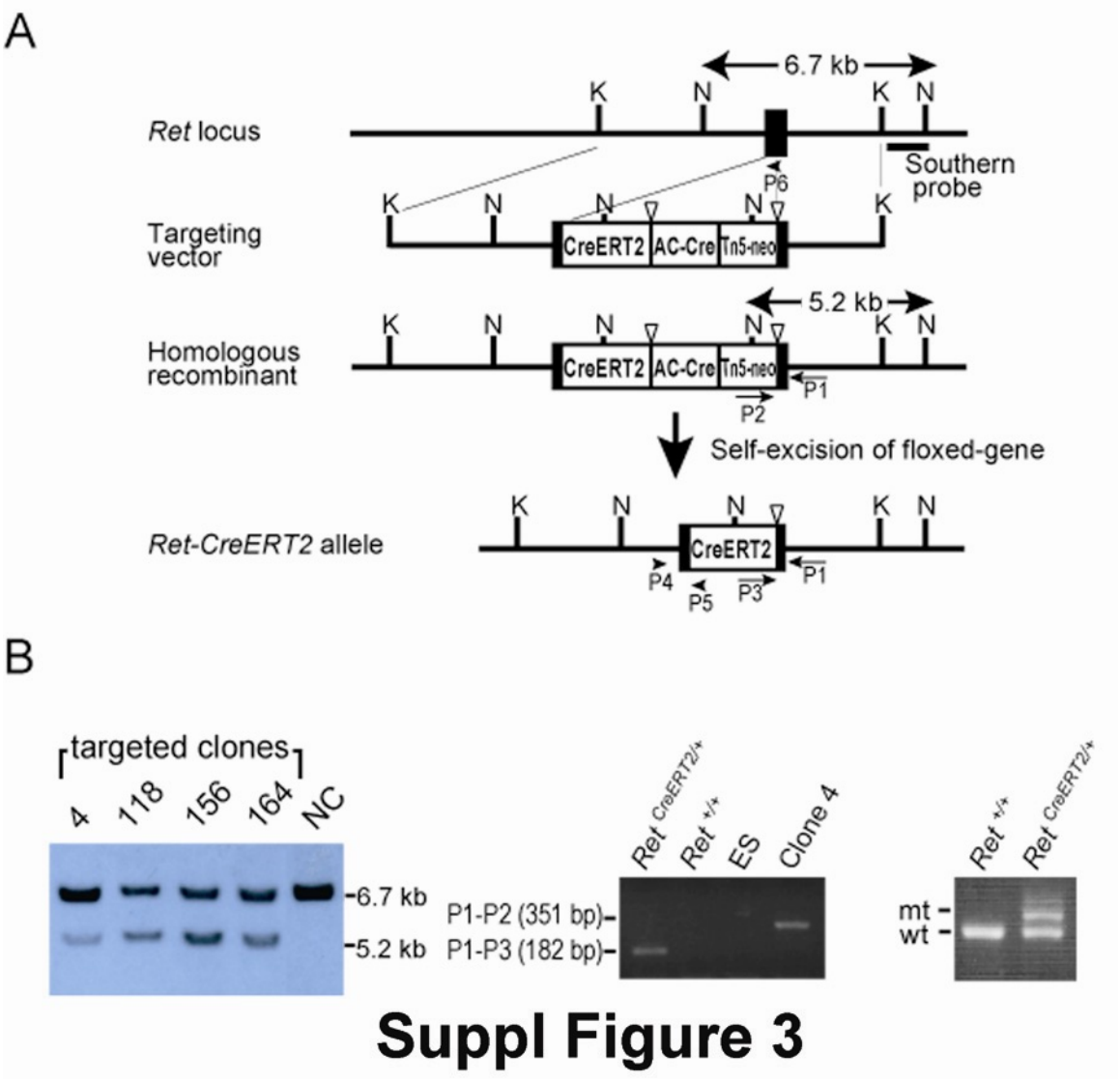

Suppl Figure 3

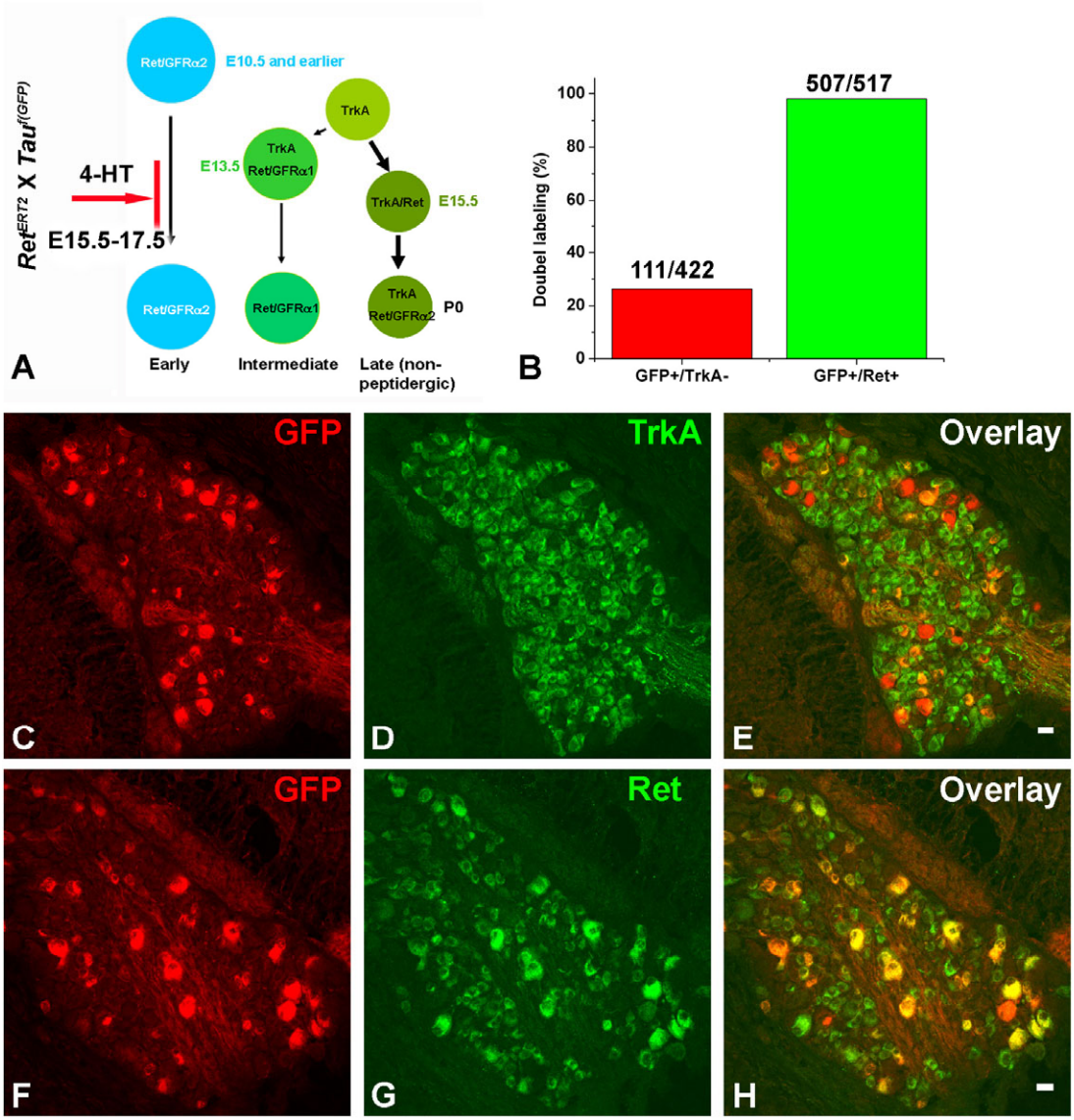

Suppl Figure 4

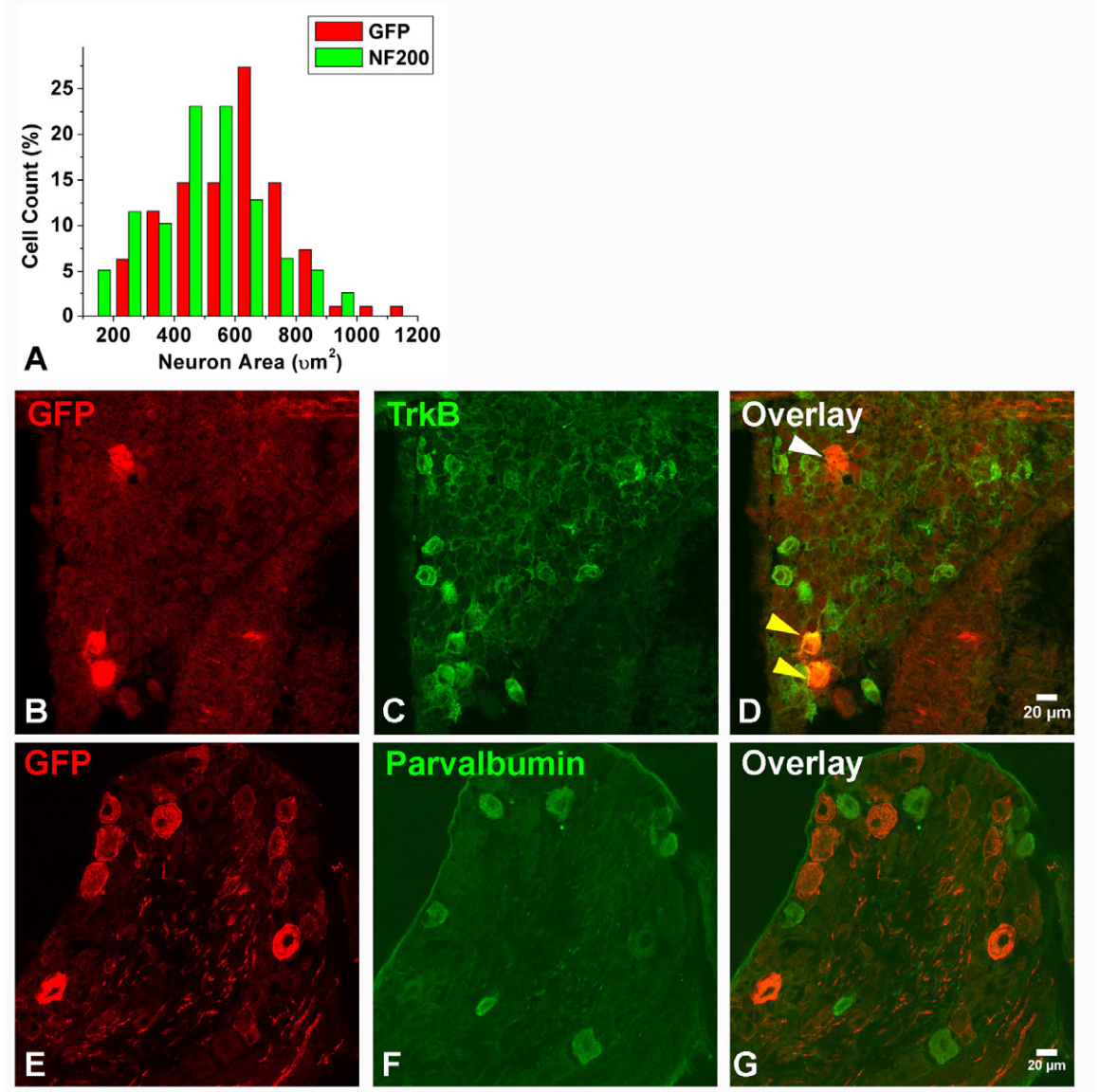

Suppl Figure 5

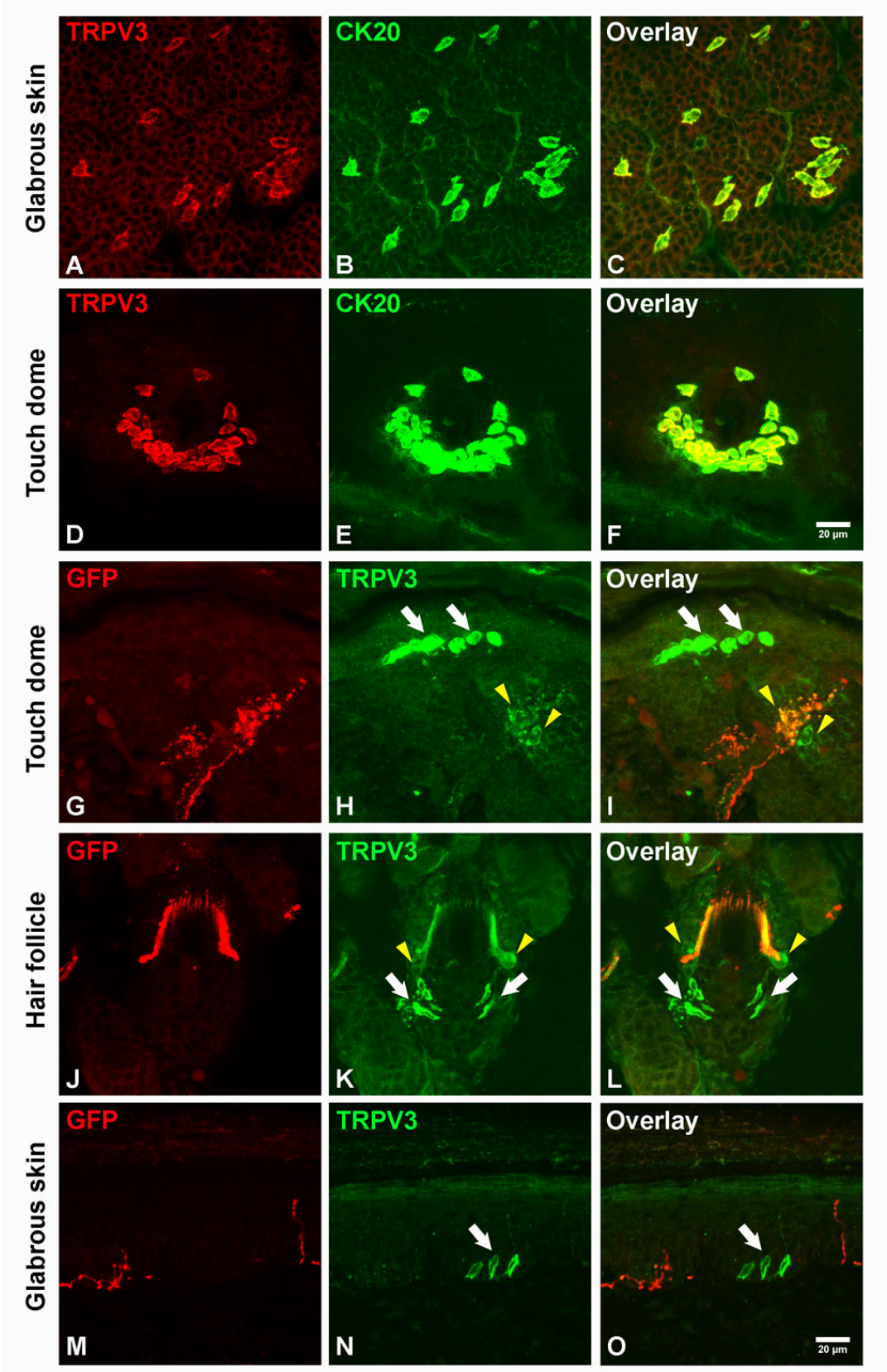

Suppl Figure 6

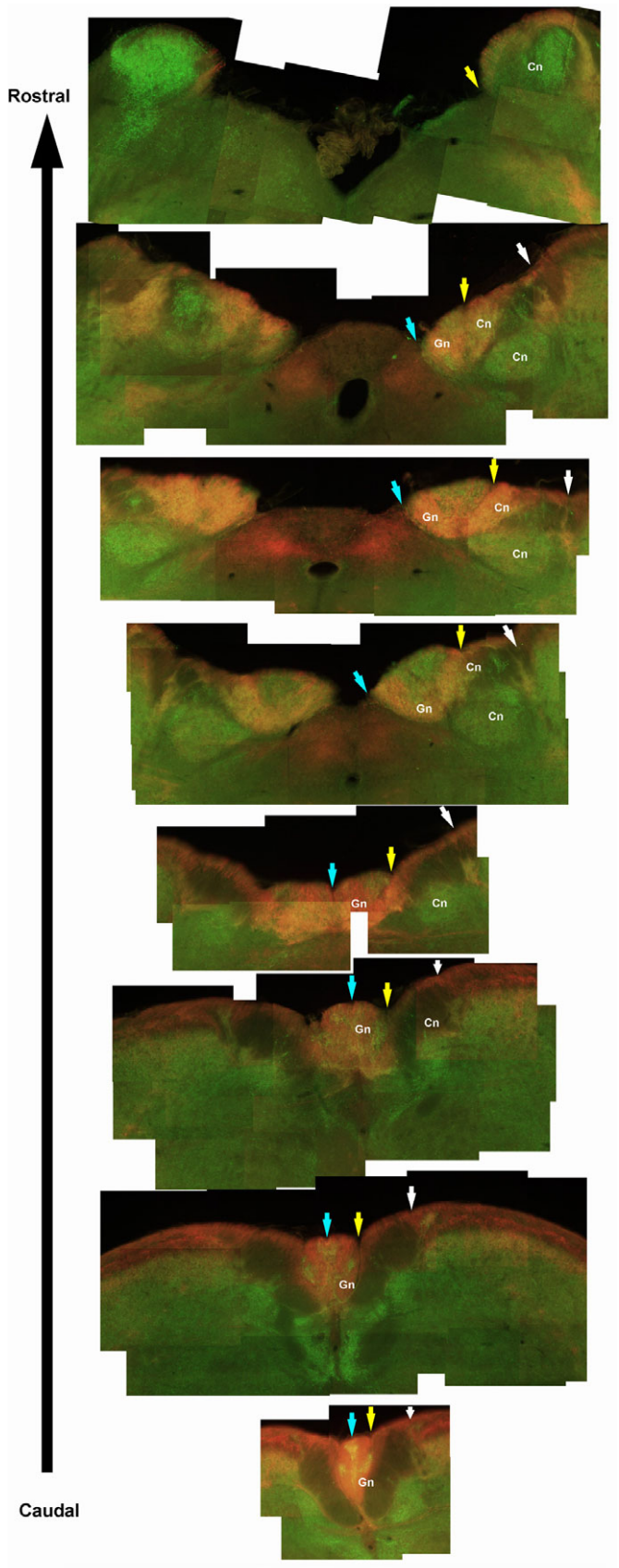

Suppl Figure 7

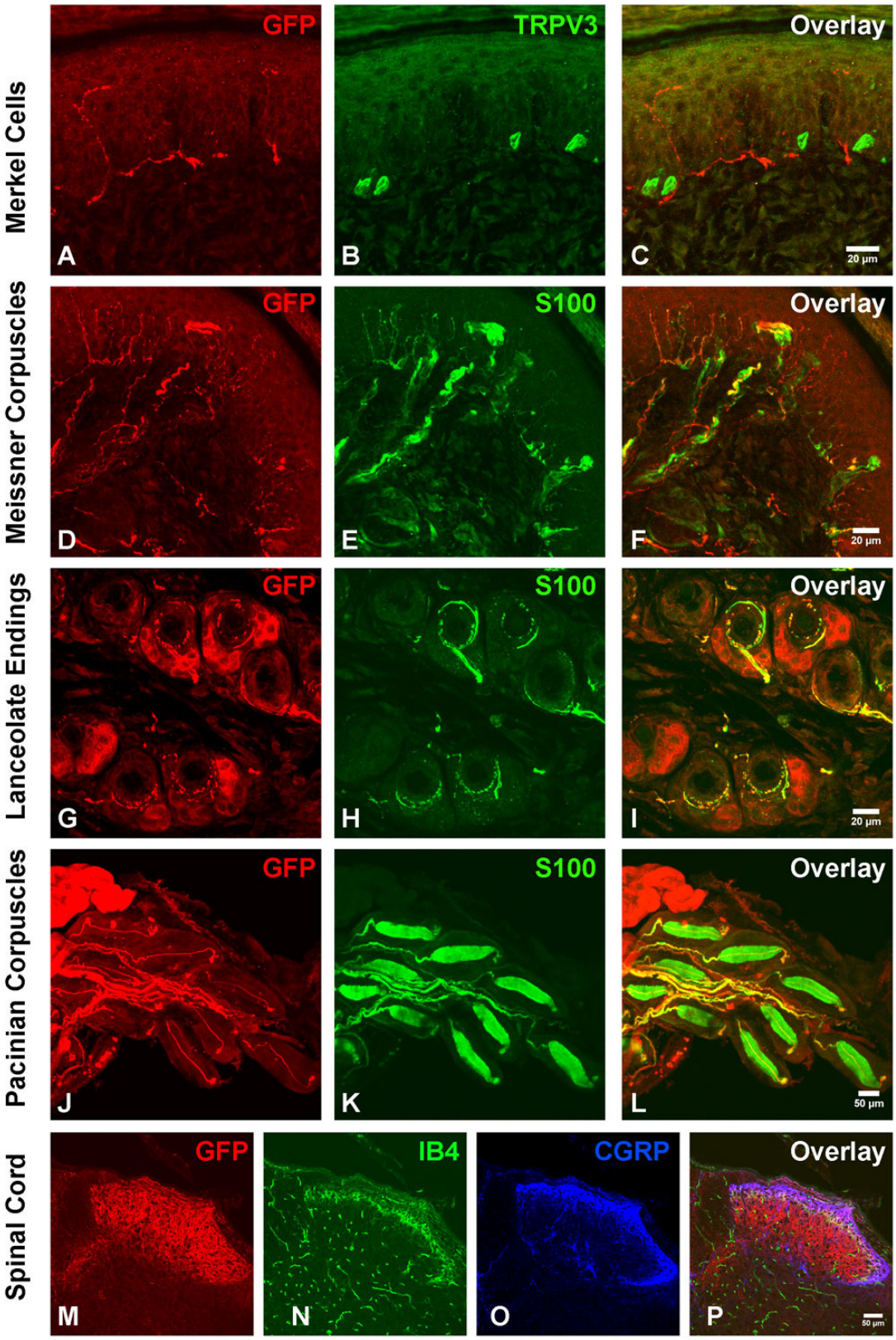

Suppl Figure 8

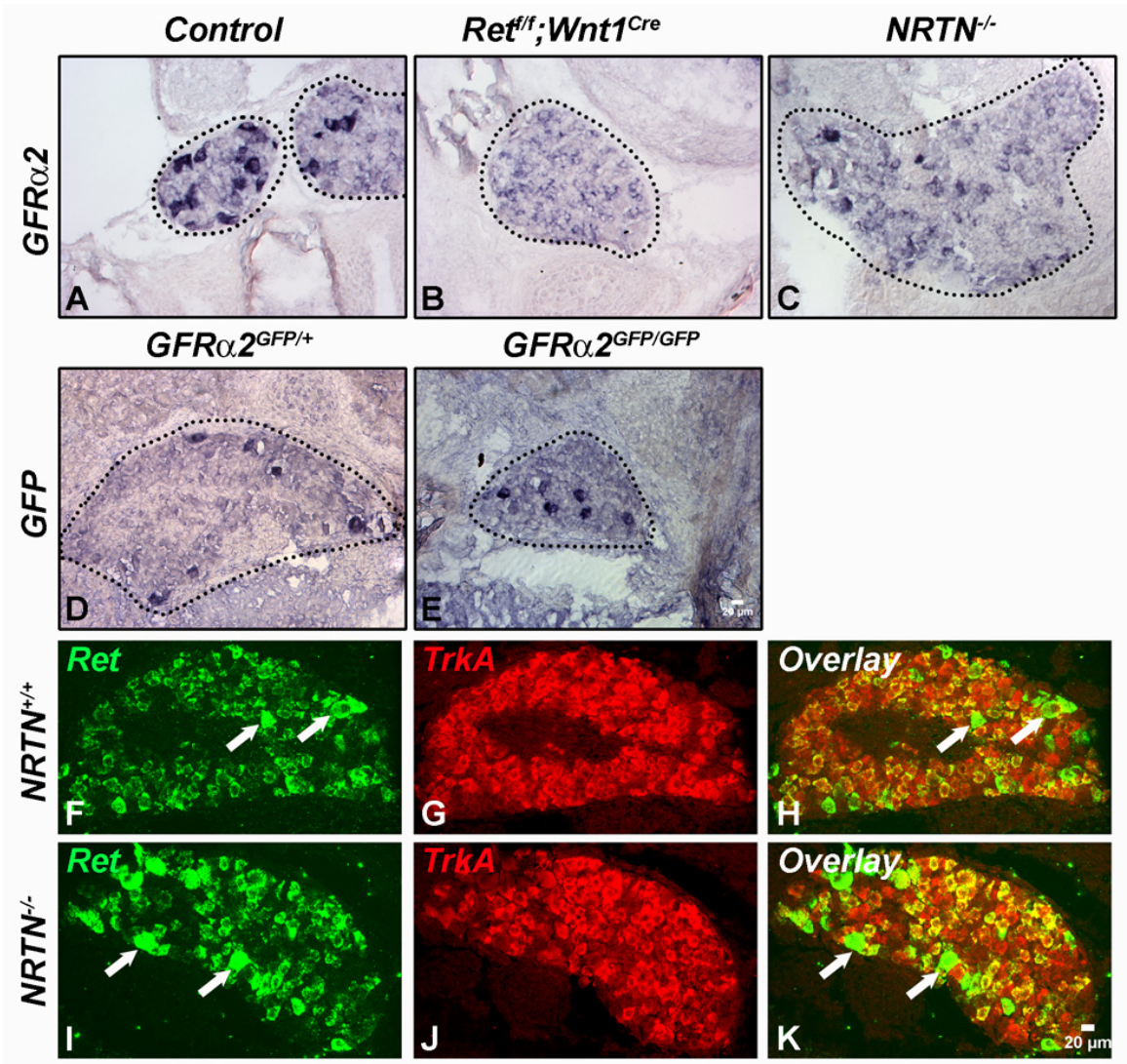

Suppl Figure 9

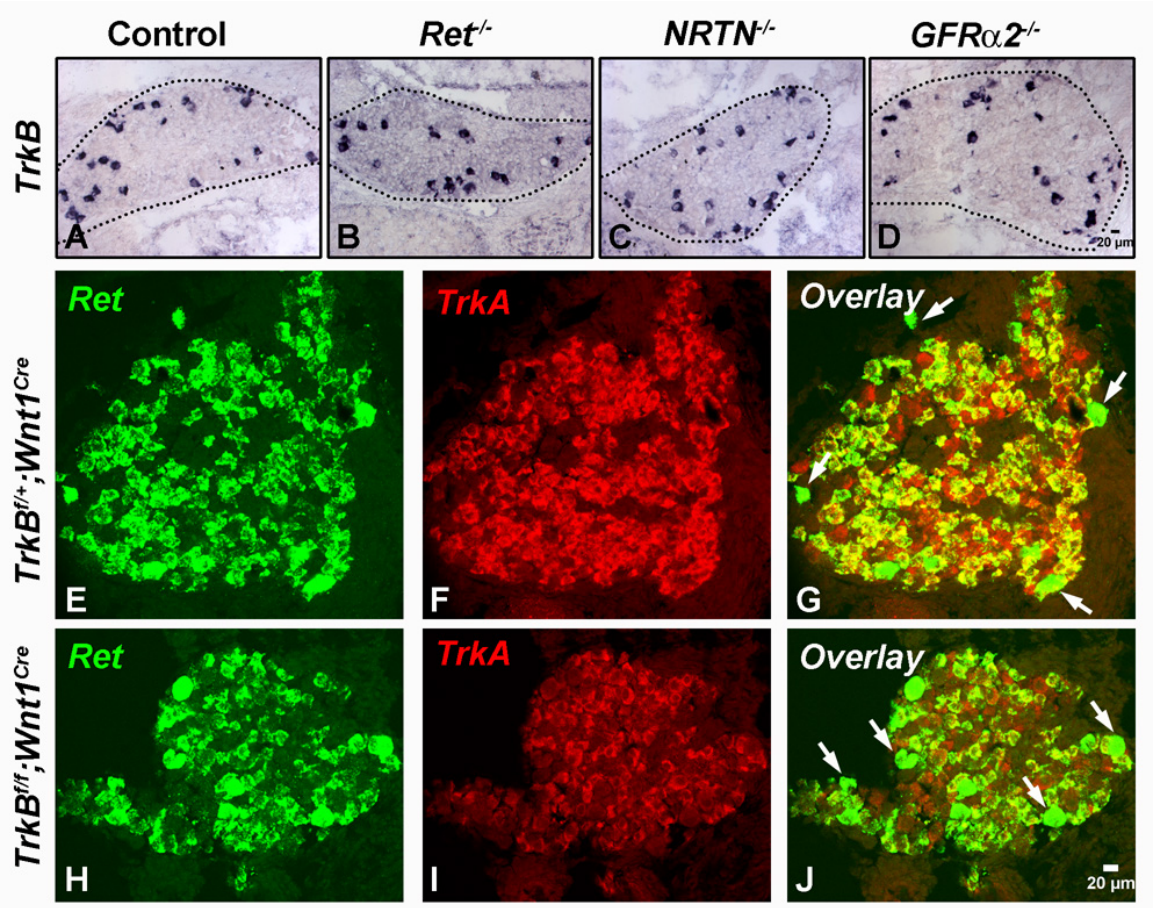

Suppl Figure 10

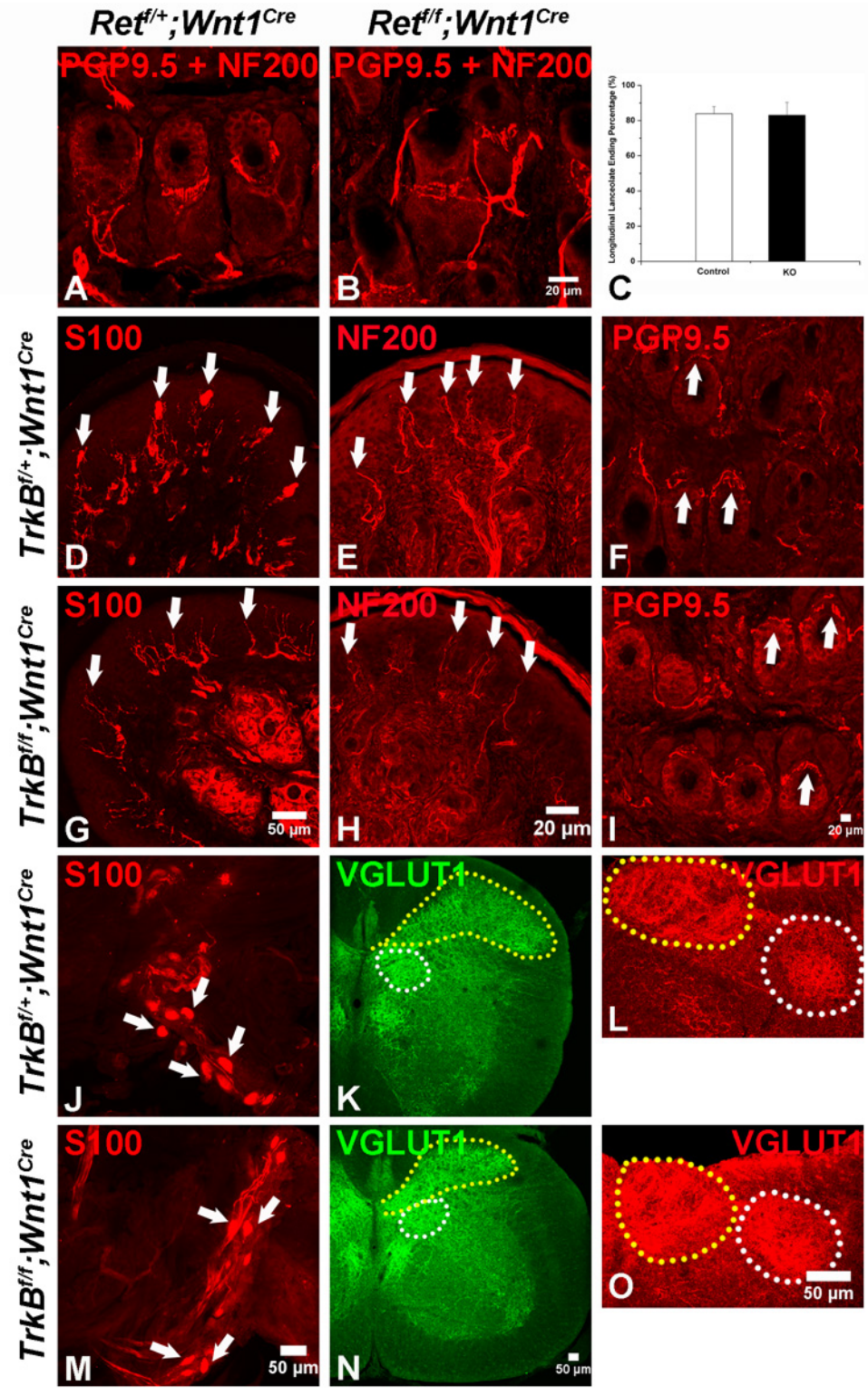

Suppl. Figure 11

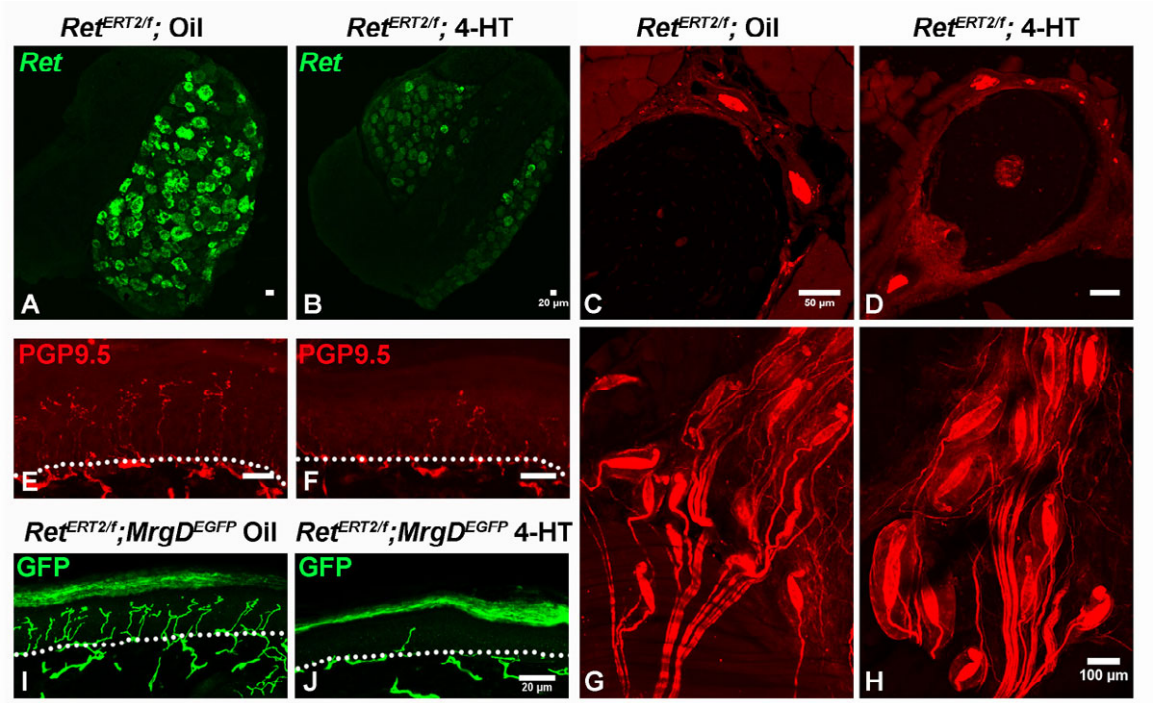

Suppl Figure 12

Supplemental Figure Legends:

Supplemental Figure 1. Developmental history of the early Ret$^+$ DRG neurons.

A-C: *In situ* hybridization of *TrkC*, *Ret* and *TrkA* using sections from wildtype lumbar DRGs at E10.5. Note the presence of large diameter, *Ret*$^+$ DRG neurons at this time when expression of *TrkA* is barely detectable. D-F: Double fluorescent *in situ* hybridization of *Ret* and *TrkA* using wildtype lumbar DRGs at E13.5. There are two populations of *Ret*$^+$ DRG neurons at this time: large-diameter Ret$^+$/TrkA$^-$ neurons (72.1%) and small-diametered Ret$^+$/TrkA$^+$ neurons (27.9%) ; some of the latter group are indicated by white arrows. G-I: Double fluorescent *in situ* hybridization of *Ret* and *TrkC* of wildtype lumbar DRGs at E13.5. There is no overlap between Ret$^+$ and TrkC$^+$ neurons at this time. J-L: Double fluorescent *in situ* hybridization of *Ret* and *TrkB* with *TrkA* null lumbar DRGs at E13.5. All Ret$^+$ neurons in *TrkA* null DRGs are early Ret$^+$ DRG neurons. There are 9 ± 3 Ret$^+$ neurons/DRG, 5 ± 2 Ret$^+$/TrkB$^+$ neurons/DRG, and 20 ± 2 TrkB$^+$ neurons/DRG. As a result, 54.3% ± 13.4% early Ret$^+$ neurons express TrkB, while 25.1 ± 7.4% TrkB$^+$ DRG neurons express Ret. N=2 for wildtype embryos at each developmental stage, and n=3 for E13.5 *TrkA*$^{-/-}$ embryos. .

Supplemental Figure 2. GFRα2 is the only Ret co-receptor expressed in early *Ret*$^+$ DRG neurons at P0.

A-C: Double fluorescent *in situ* hybridization of *Ret* and *Gfrα2* on sections of P0 wild type lumbar DRGs. Note that *Gfrα2* is expressed in only a few large-diameter, high *Ret* expressing neurons, although *Ret* itself is expressed more broadly. These large-diameter high *Ret* expressing neurons are the early *Ret*$^+$ DRG neurons. D-F: Fluorescent *in situ*

hybridization of *Ret* and *TrkA* using adjacent sections. Note that *Gfrα2*$^{+}$ neurons are *TrkA*$^{-}$, further supporting the conclusion that these large-diameter *Gfrα2*$^{+}$ neurons are the early *Ret*$^{+}$ DRG neurons. G-I: Double fluorescent *in situ* hybridization of *Ret* and *Gfrα2* using P0 *TrkA*$^{-/-}$ DRGs. The expression of *Gfrα2* is in complete overlap with that of *Ret*, which suggests that GFRα2 is the Ret co-receptor in the early Ret^{+} DRG neurons at P0. J-L: *In situ* hybridization of *Ret*, *Gfrα1* and *Gfrα2* in control and *TrkA*$^{-/-}$ lumbar DRGs at P0. The number of Ret^{+} neurons is greatly reduced (106 ± 20 neurons/section vs. 8 ± 2 neurons/section) and GFRα1^{+} neurons are completely absent (21 ± 3 neurons/section vs. 0 neurons/section) whereas the number of large-diameter GFRα2^{+} neurons are comparable (9 ± 1 neurons/section vs. 8 ± 1 neurons/section) in P0 wildtype and *TrkA*$^{-/-}$ DRGs. In addition, the number of Ret^{+} neurons in *TrkA*$^{-/-}$ mice approximately matches that of GFRα2^{+} neurons in wildtype animals. Similar results were found in *NGF*$^{-/-}$*; Bax*$^{-/-}$ mice (Luo et al., 2007). N = 2 for wildtype and n = 3 for *TrkA*$^{-/-}$ mice.

Supplemental Figure 3. Generation of the *Ret*^{ERT2} mouse line

A: Generation of the *Ret*^{ERT2} allele. The black box indicates the first exon of the *Ret* gene. White boxes and triangles depict gene expression units and *loxP* sites, respectively. Abbreviations: K; KpnI, N; NcoI B: Left; Southern blot analysis of homogonously recombined clones (left 4 lanes). NC: negative control. Middle: PCR analysis (primers, P1, P2 and P3 indicated by small arrows in the panel A) demonstrating an excision of floxed-[AC-Cre with Tn5-neo] in the *Ret* $^{CreERT2/+}$ mouse. Right: PCR genotyping of the *Ret* $^{CreERT2/+}$ mouse. Locations of the primers, P3, P4 and P5, are shown by arrowheads in the panel A.

Supplemental Figure 4. Labeling of all types of Ret$^+$ DRG neurons following treatment of *Ret^{ERT2};Tau$^{f(mGFP)}$* mice with 4-HT from E15.5 to E17.5.

A: Illustration of the late 4-HT treatment strategy. Administration of 4-HT from E15.5 to E17.5 is predicted to label all types of Ret$^+$ neurons in *Ret^{ERT2};Tau$^{f(mGFP)}$* mice. B. Quantification of GFP$^+$/TrkA$^-$ and GFP$^+$/Ret$^+$ neurons in P0 *Ret^{ERT2};Tau$^{f(mGFP)}$* mice that received the late 4-HT treatment (E15.5 to E17.5). In contrast to that seen following the early (E10.5 to E12.5) 4-HT treatment, only 26.3% GFP$^+$ neurons receiving the late 4-HT treatment are TrkA$^-$ while 98.1% of them are Ret$^+$, showing that late 4-HT treatment leads to GFP expression in many Ret$^+$/TrkA$^+$ neurons. Quantifications were made using lumbar DRG sections from three animals. Examples of double staining are shown in C-H. C-E: Double staining of GFP and TrkA with P0 lumbar DRGs of *Ret^{ERT2};Tau$^{f(mGFP)}$* mice. Note that there are two populations of GFP$^+$ neurons: most GFP$^+$ neurons are TrkA$^+$, while a few large-diameter GFP$^+$ neurons are TrkA$^-$. D-F: Double staining of GFP and Ret using P0 lumbar DRGs of *Ret^{ERT2};Tau$^{f(mGFP)}$* mice. Almost all GFP$^+$ neurons are Ret$^+$. N=3 from two litters. Scale bar: 20μm.

Supplemental Figure 5. Select labeling of the Early Ret$^+$ DRG neurons following treatment of *Ret^{ERT2};Tau$^{f(mGFP)}$* mice with 4-HT from E10.5 to E12.5.

A: Size distribution of GFP-labeled early Ret$^+$ DRG neurons and NF200$^+$ neurons, which are medium to large-diameter myelinated DRG neurons. Note that the distribution of sizes of GFP$^+$ cells peaks between 600μm^2 to 700μm^2 whereas that for NF200$^+$ neurons peaks between 400μm^2 to 600μm^2; this indicates that the early Ret$^+$ DRG neurons are

large-diameter neurons. B-D: Double staining of GFP and TrkB at P0. The white arrowhead points to a $GFP^+/TrkB^-$ neuron, while the yellow arrowheads point to two $GFP^+/TrkB^+$ neurons. Overall, 73±11% of GFP^+ DRG neurons are $TrkB^+$ at this age. E-G: Double staining of GFP and Parvalbumin at P14. There is no overlap between GFP^+ and $Parvalbumin^+$ neurons. N = 3 for P0 $Ret^{ERT2};Tau^{f(mGFP)}$ pups, and n=4 for P14 $Ret^{ERT2};Tau^{f(mGFP)}$ animals from two litters.

Supplemental Figure 6. GFP-labeled early Ret^+ DRG neurons do not innervate Merkel cells.

A-C: Whole mount staining of a P14 footpad using rabbit anti-TRPV3 and mouse anti-CK20 antibodies. D-F: Double staining using TRPV3 and CK20 antibodies with P0 back hairy skin sections. Note that in both the footpad and touch domes, the staining patterns observed with the TRPV3 antibody is the same as that found with the CK20 antibody, which is a Merkel cell specific marker (Moll et al., 1996). This is relevant because the CK20 antibody cannot be used for double labeling experiments with mGFP due to incompatible fixation conditions, while the TRPV3 antibody can. Thus, in subsequent experiments, TRPV3 and GFP double labeling was performed to determine whether GFP^+ axonal endings are associated with Merkel cells. G-O: Double staining of GFP and TRPV3 in the skin of $Ret^{ERT2};Tau^{f(mGFP)}$ mice that had been treated with 4-HT from E10.5 to E12.5. G-I: P0 back hairy skin. Note that GFP fibers are present but do not innervate Merkel cells (white arrows) in this touch dome. These GFP^+ fibers are most likely immature longitudinal lanceolate endings (Peters et al., 2002) that are affiliated with weakly $TRPV3^+$ immature terminal Schwann cells (yellow arrowheads, see J-L). J-

L: P14 guard hair follicle. Note that GFP^+ fibers terminate as a palisade of longitudinally oriented lanceolate endings that are lined with$TRPV3^+$ terminal glia (yellow arrowheads). The palisade surrounds the follicle and is capped by a sebeacceous gland. $TRPV3^+$ Merkel cells (white arrows) located in the follicle and below the palisade are not contacted by GFP^+ axons. M-O: P14 regular glabrous skin. Here again, GFP^+ fibers are not associated with Merkel cells (white arrow). N = 3 for P0 $Ret^{ERT2};Tau^{f(mGFP)}$ pups, and n=4 for P14 $Ret^{ERT2};Tau^{f(mGFP)}$ animals from two litters.

Supplemental Figure 7. Central projections of RA mechanoreceptors innervate the gracile and cuneate nuclei of medulla.

Shown are serial sections through the medulla of a two month old $Ret^{ERT2};Tau^{f(mGFP)}$ mouse treated with 4-HT at E11.5 and E12.5. Representative medulla sections are arranged from caudal (bottom) to rostral (top). RA mechanoreceptors are labeled with GFP in this mouse, and thus their central projections into gracile and cuneate nuclei are visualized using GFP antibody staining (red). On the other hand, the entire gracile and cuneate nuclei are visualized by VGLUT1 staining (green). The middle boundary of the gracile nucleus is indicated by a blue arrowhead, the lateral boundary of the gracile nucleus (which is also the boundary between the gracile and the cuneate nuclei) is indicated by a yellow arrow, and the lateral boundary of the cuneate nucleus is indicated by a white arrow. The locations of gracile and cuneate nuclei are also confirmed using $Avil^{AP}$ mice (Hasegawa et al., 2007), in which all somatosensory neurons are labeled with hPLAP (data not shown). Note that GFP^+ fibers only terminate in subdomains of gracile

and cuneate nuclei. Similar results were found with P14 $Ret^{ERT2};Tau^{f(mGFP)}$ mice (n=2). N=2 for two-month old animals.

Supplemental Figure 8. Peripheral and central projection of early Ret$^+$ neurons in $Ret^{f(CFP)};Wnt1^{Cre}$ mice.

A-C: Double immunostaining for GFP and TRPV3. Note that GFP$^+$ fibers do not innervate Merkel cells in glabrous skin. D-E: Double staining of GFP and S100 in the footpad. Note that GFP$^+$ fibers form a Meissner corpuscle. G-H: Double staining of GFP and S100 in the back hairy skin of the foot. Note that GFP$^+$ fibers form lanceolate endings. J-L: Double staining of GFP and S100 in the periosteum membrane. Note that a single GFP$^+$ fiber innervates each Pacinian corpuscle. M-P: Triple staining of GFP, CGRP and IB4 using sections of the thoracic spinal cord. Note that GFP$^+$ fibers innervate layer I to V of spinal cord. N=3 for P14 $Ret^{f(CFP)};Wnt1^{Cre}$ mice.

Supplemental Figure 9. NRTN-GFRα2/Ret signaling is not required for neonatal survival of RA mechanoreceptors.

A-C: In situ hybridization of *Gfrα2* in P0 control, $Ret^{f/f};Wnt1^{Cre}$, and *Nrtn* null lumbar DRGs. Note that the number of large diameter, strongly GFRα2$^+$ neurons is much less in both $Ret^{f/f};Wnt1^{Cre}$ and *Nrtn* lumbar DRGs. D-E: *In situ* hybridization of *Gfp* in P0 $Gfr\alpha2^{GFP}$ knock-in heterozygous and homozygous lumbar DRGs (5± 1/section vs. 4 ± 1/section). C-H: Double fluorescent *in situ* hybridization for *Ret* and *TrkA* in control and *Nrtn* null lumbar DRGs at P0 (Ret$^+$/TrkA$^-$ neuron number: 10 ± 1/section vs. 9 ± 1/section). Examples of large-diameter Ret$^+$/TrkA$^-$ neurons are indicated by the white

arrows. N = 3 for P0 *Ret$^{f/f}$;Wnt1^{Cre}* pups, n = 5 for P0 *Nrtn* null pups, and n = 3 for P0 *Gfrα2^{GFP}* homozygous knock-in pups.

Supplemental Figure 10. RA mechanoreceptors are present in the absence of Ret signaling components or *TrkB* at P0.

A-D: In situ hybridization of *TrkB* in P0 control, *Ret$^{f/f}$;Wnt1^{Cre}*, *Nrtn* null, and *Gfrα2* null lumbar DRGs. At least some of the TrkB^{+} neurons at P0 are RA mechanoreceptors. Interestingly, almost identical numbers of TrkB^{+} neurons are found in control and mutant mice. Control: 21 ± 3/ DRG section, *Ret$^{f/f}$;Wnt1^{Cre}*:21 ± 3/ DRG section, *Nrtn* null: 21 ± 5/DRG section and *Gfrα2* null: 20 ± 4/DRG section. N≥3 for each genotype. E-J: *Ret/TrkA* double fluorescent *in situ* hybridization using P0 control (E-G) or *TrkB* mutant (H-J) lumbar DRGs. Ret^{+}/TrkA^{-} neurons are considered to be the RA mechanoreceptors. There are 6 ± 2 and 5 ± 2 Ret^{+}/TrkA^{-} neurons in the control and *TrkB* mutant DRGs respectively.

Supplemental Figure 11. *TrkB* is required for the formation of Meissner corpuscles and longitudinal lanceolate endings, but not Pacinian corpuscles or central projections of mechanoreceptors.

A-B: High magnification image of lanceolate endings in P14 control and *Ret$^{f/f}$;Wnt1^{Cre}* mice. Note that while the morphologies of longitudinal lanceolate endings are disorganized, the percentage of hair follicles associated with these endings is comparable in control and mutant mice (C). N=3 for both genotypes. D, G: Meissner corpuscle staining using anti-S100 antibody for control and *TrkB$^{f/f}$;Wnt1^{Cre}* footpads at P14. Note

the lack of corpuscles in the *TrkB$^{f/f}$;Wnt1^{Cre}* footpad. Meissner corpuscles in the wild type footpad are indicated by white arrows, while in the mutant footpad the white arrows indicate the approximate locations where Meissner corpuscles should be present. E,H: Staining of control and *TrkB$^{f/f}$;Wnt1^{Cre}* footpads using the NF200 antibody. NF200^{+} axons are present in the dermal papillae of *TrkB$^{f/f}$;Wnt1^{Cre}* mice (white arrows), although the corpuscle is not formed. F,I: Staining of longitudinal lanceolate endings (white arrows) PGP9.5 and NF200 antibodies in control and *TrkB$^{f/f}$;Wnt1^{Cre}* mice. Longitudinal lanceolate endings may be slightly disorganized in the absence of *TrkB*. J, M: Whole-mount Pacinian corpuscle (white arrows) staining using the S100 antibody. The number and morphology of Pacinian corpuscles in *TrkB$^{f/f}$;Wnt1^{Cre}* and control mice are similar. K, N: Cervical spinal cord staining using VGLUT1 antibody. The pattern of VGLUT1 staining indicates that *TrkB$^{f/f}$;Wnt1^{Cre}* and control mice have comparable amounts of mechanosensory (yellow dot line) and proprioceptive (white dot line) synapses in the spinal cord. L, O: Medulla stained with a VGLUT1 antibody. The VGLUT1 staining pattern of the medulla indicates that the innervation of both the gracile (yellow dot line) and cuneate nuclei (white dot line) is normal in *TrkB$^{f/f}$;Wnt1^{Cre}* mice. N=3 for P14 *TrkB$^{f/f}$;Wnt1^{Cre}* mice.

Supplemental Figure 12. Acute deletion of *Ret* in adult *Ret$^{ERT2/f}$* mice, and longitudinal lanceolate endings in adult *Ret$^{f/f}$;Wnt1^{Cre}* mice.

A-B: *Ret in situ* hybridization on DRGs of *Ret$^{ERT2/f}$* mice that had been treated with either oil (vehicle) or 4-HT beginning at three weeks of age. Note that with 4-HT treatment, *Ret* is almost completely deleted in *Ret$^{ERT2/f}$* DRG neurons. C-D: Anti-S100 staining of

the periosteum membrane to visualize Pacinian corpuscles following following oil (C) or 4-HT treatment (D). Note that Pacinian corpuscles are present in normal number and with normal morphology two weeks following acute *Ret* deletion in three-week old animals. E-F: Anti-PGP9.5 staining of glabrous skin to visualize the non-peptidergic innervation in the epidermis following oil (E) or 4-HT treatment (F) of three-week old mice. After 4-HT treatment, there are fewer free nerve endings in the skin. The boundary between the epidermis and dermis is shown with the white dotted line. I-J: Anti-GFP staining of non-peptidergic fibers in glabrous skin of $Ret^{ERT2/f};MrgD^{EGFP}$ mice, which were treated with either oil (I) or 4-HT (J) beginning at three weeks of age. The boundary between epidermis and dermis is shown by the white dotted line. Consistent with the PGP9.5 staining (E-F), non-peptidergic fibers, as revealed by GFP^{+} staining, are nearly completely absent following acute *Ret* deletion in these animals. Thus, Ret signaling is required for maintenance of epidermal innervation by adult $MrgD^{EGFP+}$ non-peptidergic nociceptors. G-H: Anti-S100 staining of a whole-mount periosteum membrane six months after acute *Ret* deletion. Not that Pacinian corpuscles are present in normal number and morphology, suggesting that *Ret* is not required for the long-term maintenance of Pacinian corpuscles. N = 10 for $Ret^{ERT2/f}$ mice treated with 4-HT at three weeks of age. Three mice were examined two weeks after 4-HT treatment, two mice harboring the $MrgD^{GFP}$ allele were also examined two weeks after 4-HT treatment, and five mice were examined six months later. N=8 for controls.

Supplemental Materials and Methods

Mouse lines:

To generate the *Ret*-CreERT2 mouse line, a gene cassette composed of the CreERT2 cDNA (a kind gift from Pierre Chambon, (Feil et al., 1997)), intron polyA, and a floxed cassette consisting of *AC-Cre* with Tn5-neo was inserted into the endogenous promoter of the mouse *Ret* locus by gene targeting as described previously (Uesaka et al., 2008). *AC-Cre* drives expression of Cre recombinase under the control of the Angiotensin Converting-enzyme promoter, allowing self-excision of the floxed gene in the germ line (Bunting et al., 1999). Excision of floxed-[AC-Cre with Tn5-neo] was verified by PCR using primers P1 (AGCGCTAACTTCACCCCGGCCCCTA), P2 (ACGCACGGTGTTGGGTCGTTTGTTC) and P3 (CTTATCATGTCTGGATCTCGACTTCG). Genotyping of *Ret* $^{CreERT2/+}$ mouse was performed using primers P4 (CAGCGCAGGTCTCTCATCAGTACCGCA), P5 (ACTCGTTGCATCGACCGGTAATGCAGGC) and P6 (ACGTCGCTTTCGCCATCGCCCGTGCGC) (See fig 3A for the locations of all the primers). Thus, the *Ret*-CreERT2 allele is a null allele and expresses CreERT2 under the control of the genomic regulatory region of the *Ret* gene.

Mice harboring the *Ret* null allele were generated by crossing $Ret^{f/f}$ males to a germline Cre ($Sox2^{Cre}$) females (Hayashi et al., 2003). $Ret^{+/-}$ mice were then intercrossed to generate $Ret^{-/-}$ P0 pups. $TrkB^{f/f}$ mice, described previously (Chen et al., 2005), were crossed to $Wnt1^{Cre}$ mice (Danielian et al., 1998) to generate the *TrkB* conditional mutant mice ($TrkB^{f/f};Wnt1^{Cre}$). $TrkA^{LacZ}$ heterozygous mice (Moqrich et al., 2004) were

intercrossed to obtain *TrkA* null embryos and P0 pups. *NRTN* null, $GFR\alpha2^{GFP}$ and $MrgD^{EGFP}$ knock-in mouse lines were previously described (Heuckeroth et al., 1999; McDonagh et al., 2007; Zylka et al., 2005).

To analyze the central projections of RA mechanoreceptors lacking *Ret*, we crossed Ret^{ERT2} mice to either the $Ret^{f(CFP)}$ or $Tau^{f(mGFP)}$ mouse lines for 2 days, and checked for pregnancies 11 days following the first day of mating. Pregnant females were considered to be E11.5 and were gavaged with ~1mg of 4-HT per day for two days (E11.5 and E12.5). A shorter time and lower dosage of 4-HT treatment was used here to avoid massive enteric neuron death and agenesis of the kidneys, which are phenotypic of *Ret* null mice. Pups were genotyped at P0, and $Ret^{ERT2/f(CFP)}$ (*Ret* mosaic KO) or $Ret^{ERT2};Tau^{f(mGFP)}$ (control) mice were chosen for analysis at P14. For the E15.5 analysis, E11.5 $Ret^{ERT2};Tau^{f(mGFP)}$ (control) mice were gavaged with 1mg or 0.6mg of 4-HT, and E11.5 $Ret^{ERT2/f(CFP)}$ (*Ret* mosaic KO) mice were gavaged with 1mg of 4-HT

For adult *Ret* deletion experiments, Ret^{ERT2} mice were crossed with $Ret^{f/f}$ or $Ret^{f/f};MrgD^{EGFP}$ mice (Luo et al., 2007), and $Ret^{ERT2/f}$ or $Ret^{ERT2/f};MrgD^{EGFP}$ mice were chosen for treatment. Beginning at three weeks of age, mice were gavaged with either sunflower seed oil (vehicle control) or 1mg 4-HT per day for 7 consecutive days. Tissues were collected for analysis two to three weeks or six months after 4-HT treatment.

Dissection, Fixation and Immunostaining: Spinal cord, DRG and medulla section staining: P14 animals were euthanized with CO_2. The head and cervical spinal column

were cut and fixed in a solution of 4% PFA for 30min at room temperature. Then, hindbrains and cervical spinal cords were removed and fixed with 4% PFA for two hours at 4°C. Thoracic and lumbar spinal columns were directly fixed with 4% PFA for two hours at 4°C. After fixation, tissues were washed three times with PBS, incubated with 30% sucrose overnight, and embedded in O.C.T. Immunostaining of the cervical spinal cord and medulla was done using 50µm floating sections, while immunostaining of thoracic and lumbar spinal cord and DRG was done with 20µm sections. P0 spinal columns were dissected and freshly frozen in O.C.T, and 20µm sections were made from rostral to caudal levels. The whole E15.5 embryo was freshly frozen in O.C.T, and 20µm sections from tail to head were prepared. All immunostaining steps were as previously described (Luo et al., 2007). For E15.5 central projection analysis, thoracic or lumbar spinal columns were fixed in 4% PFA for 4 hours at 4 °C. The whole thoracic spinal cord and DRGs were then dissected, cut in the middle from the dorsal to ventral side, incubated with 30% sucrose overnight, and embedded in O.C.T. 50µm saggital spinal cord sections and the lateral spinal cord with attached thoracic DRGs were collected and processed with anti-GFP immunostaining. GFP^+ neurons were counted in every stained DRG.

Glabrous and hairy skin staining: Hindpaw footpads, paw back hairy skin, and back hairy skin were dissected after euthanizing animals, and then fixed in 4% PFA overnight at 4°C. Footpads were sectioned perpendicular to the surface, while hairy skin was sectioned parallel or obliquely to the surface. Footpads were sectioned (20µm) and all sections were collected. Usually, sections from one hindpaw footpad were used for

Meissner corpuscle staining, and those of the other footpad were used for Merkel disc staining. Alternatively, footpads and hairy skin were analyzed using 30µm floating sections. Meissner corpuscles and lanceolate endings in the feet were visualized by S100 immunostaining, Merkel discs in glabrous and hairy skin were visualized by TRPV3 immunostaining, and lanceolate endings in the hairy skin were immunostained using a combination of PGP9.5 and NF200 antibodies.

Merkel cell whole-mount staining: Dissected footpads were incubated in a solution containing 2M sodium bromide for 1 hour at room temperature, and the epidermis was carefully separated from the dermis. The isolated epidermal samples were then fixed with cold acetone for 10 minutes at -20°C, dried, rinsed with PBS, and incubated with antibodies diluted in PBS (method adapted from Dr. Robin Krimm, personal communication).

DRG and Pacinian corpuscle whole mount staining: L5 DRGs or distal interosseus membranes were dissected after euthanizing animals, postfixed in 4% PFA overnight at 4°C, washed three times with PBS containing 1% Triton and 1% Tween 20, and incubated in the same buffer containing primary antibodies (L5 DRGs, rabbit anti-GFP, Pacinian corpuscles, rabbit anti-S100, with or without chicken anti-GFP) overnight at room temperature. On the next day, DRGs or interosseus membranes were washed three times with PBS containing 1% Tween 20 for one hour each, and then stained with secondary antibody overnight at room temperature. On the third day, tissues were washed three times with PBS containing 1% Tween 20 for one hour each, and passed

through glycerol serial solutions for clearing and then mounted. Usually, 35 ± 5 Pacinian corpuscles were found within each interosseus membrane.

Pacinian corpuscle sectioning and staining: The distal halves of mouse legs were dissected, postfixed in 4% PFA overnight at 4°C, and then decalcified using a solution containing formic acid (22%) and sodium citrate (10%) for two days at 4°C. Tissues were sectioned (20μm) continuously from the ankle towards the knee. Pacinian corpuscles were visible in the interosseus membrane at the level where the fibula and tibia begin to separate, determined by either light microscopy or S100 staining.

Primary antibodies used in this study are: chicken anti-GFP (Aves Labs GFP-1020, 1:1000), rabbit anti-GFP (Invitrogen, A11122, 1:1000), rabbit anti-CGRP (Millipore, AB5920, 1:1000), Alexa 488-conjugated IB4 (Invitrogen, 1:200), rabbit anti-TrkA (Millipore, AB1577, 1:1000), rabbit anti-NF200 (Millipore, AB1982, 1:1000), rabbit anti-PGP9.5 (Millipore, AB1761 ASR, 1:1000), rabbit anti-TrkB (a gift from Dr Louis Reichardt, UCSF, 1:1000), rabbit anti-TRPV3 (a gift from Dr. Michael Caterina, JHU, 1:200) , mouse anti-CK20 (Dako, M7019, 1:20), rabbit anti-S100 (Dako, Z0311, 1:400), rabbit anti-Ret (Immuno-Biologcial Laboratories, 18121, 1:20), rabbit anti-GFRα2 (R & D system, AF429, 1:50), rabbit anti-Parvalbumin (Swant, PV28, 1:200), and guinea pig anti-VGLUT1 (Millipore, AB5905, 1:1000). Secondary antibodies are: Alexa 546 conjugated goat anti-chicken antibody, Alexa 488 or 546 conjugated goat anti-rabbit antibody, Alexa 488 conjugated goat anti-mouse antibody, Alexa 488 or 546

conjugated goat anti-guinea pig antibody. All secondary antibodies were purchased from Invitrogen.

In situ hybridization and double fluorescent in situ hybridization: In brief, fresh frozen DRG sections were postfixed with 4% PFA for 20 minutes, treated with a solution containing 0.1% DEPC (Sigma) for 5 minutes, then a solution containing 25mg/ml proteinase K (Invitrogen) for 5 minutes, followed by acetylation for 10 minutes. Sections were pre-hybridized for 30min, and then hybridized with the corresponding probe (1-2ng/ul) overnight at 62°C. On the next day, sections were washed with 2xSSC for 3 X 30 minutes at 65°C, and then subjected to anti-DIG-AP conjugated antibody (Roche) staining and a BCIP/NBT (Roche) color reaction. Double-fluorescent *in situ* hybridizations were done using a combination of DIG-labeled and fluorescein-labeled *cRNA* probes. All other procedures were similar to that of single probe *in situ* hybridizations except for the antibody detection and color reaction steps. After washing with 2 X SSC, anti-DIG-AP conjugated antibody was added to sections for 2 to 3 hours at room temperature. Then, an HNPP/fast red detection kit (Roche) was used for the AP red fluorescent color reaction. Then, an anti-FITC-POD conjugated antibody (Roche) was used to detect the FITC labeled probe, and a TSA plus fluorescein system (PekinElmer NEL741001KT) was used for the POD green fluorescence color reaction.

Hematoxylin and Eosin (H & E) staining: Mouse spinal cord or leg sections were washed with tap water for 2 minutes, stained with a hemoxylin solution (Sigma, GHS132) for 10 minutes, washed with tap water again, and stained with an Eosin Y solution

(Sigma, HT110132, for leg sections, use 1: 2 diluted Eosin Y solution in 70% ethanol for just one to two dips, while for spinal cord sections, use undiluted Eosin Y solution for two minutes). Then, samples were dehydrated with serial ethanol solutions and xylene, and mounted with DPX mountant for histology (Sigma 44581).

Image analysis and quantification: All image analysis was done using Image J software.

Area measurements of GFP-labeled neurons: Images taken with 20x magnification were imported into Image J. GFP^+ DRG neurons were outlined, and the areas of all GFP^+ DRG neurons were measured.

Quantification of percentage of longitudinal lanceolate endings in a population of hair follicles: We used hindpaw back hairy skin for this analysis because most hair follicles in this region are innervated by longitudinal lanceolate endings. Hair follicles observed to exhibit a lack of staining in their center and containing a surrounding sebaceous gland were scored because longitudinal lanceolate endings can only be found when follicles are in this plane of section. About 80% to 90% of wildtype hair follicles in this plane of section have longitudinal lanceolate endings. Fewer hair follicles with this profile were found in the Ret mutant mice because their hair follicles are smaller. Nevertheless, 80% to 90% of hair follicles displaying this profile in Ret mutant mice are associated with longitudinal lanceolate endings.

Quantification of spinal cord, dorsal column, and medulla innervation in $Ret^{f/f};Wnt1^{Cre}$, $Ret^{ERT2};Tau^{mGFP}$ and $Ret^{ERT2/f(CFP)}$ mice: To measure the spinal cord and dorsal column signal intensity, the innervated area was outlined and measured, which gave area and mean raw signal. In addition, a non-innervated area nearby is also outlined and measured, which gives the mean background. The total signal was then calculated by area * (mean raw signal- mean background). The average signal of $Ret^{ERT2/f(CFP)}$ spinal column and dorsal column were considered as "1" (baseline), and the values of total signals in $Ret^{ERT2};Tau^{mGFP}$ mice were normalized accordingly. The mean, standard deviation and standard error were then calculated according to the normalized values. For medulla innervation, the relative area occupied by GFP^+ fibers within gracile and cuneate nucleus was quantified. Basically, the gracile and cuneate nuclei are identified by vGlut1 staining, and their areas were measured. On the same section, GFP^+ fiber innervated areas within gracile and cuneate nuclei were also measured, and the relative occupied area was calculated by GFP^+ fiber area/gracile or cuneate nucleus area. The mean, standard deviation and standard error were calculated using this relative value. The student *t* test was used for calculating the P value.

References:

Bunting, M., Bernstein, K. E., Greer, J. M., Capecchi, M. R., and Thomas, K. R. (1999). Targeting genes for self-excision in the germ line. Genes Dev *13*, 1524-1528.

Chen, X., Ye, H., Kuruvilla, R., Ramanan, N., Scangos, K. W., Zhang, C., Johnson, N. M., England, P. M., Shokat, K. M., and Ginty, D. D. (2005). A chemical-genetic approach to studying neurotrophin signaling. Neuron *46*, 13-21.

Danielian, P. S., Muccino, D., Rowitch, D. H., Michael, S. K., and McMahon, A. P. (1998). Modification of gene activity in mouse embryos in utero by a tamoxifen-inducible form of Cre recombinase. Curr Biol *8*, 1323-1326.

Feil, R., Wagner, J., Metzger, D., and Chambon, P. (1997). Regulation of Cre recombinase activity by mutated estrogen receptor ligand-binding domains. Biochem Biophys Res Commun *237*, 752-757.

Hasegawa, H., Abbott, S., Han, B. X., Qi, Y., and Wang, F. (2007). Analyzing somatosensory axon projections with the sensory neuron-specific Advillin gene. J Neurosci *27*, 14404-14414.

Hayashi, S., Tenzen, T., and McMahon, A. P. (2003). Maternal inheritance of Cre activity in a Sox2Cre deleter strain. Genesis *37*, 51-53.

Heuckeroth, R. O., Enomoto, H., Grider, J. R., Golden, J. P., Hanke, J. A., Jackman, A., Molliver, D. C., Bardgett, M. E., Snider, W. D., Johnson, E. M., Jr., and Milbrandt, J. (1999). Gene targeting reveals a critical role for neurturin in the development and maintenance of enteric, sensory, and parasympathetic neurons. Neuron *22*, 253-263.

Luo, W., Wickramasinghe, S. R., Savitt, J. M., Griffin, J. W., Dawson, T. M., and Ginty, D. D. (2007). A hierarchical NGF signaling cascade controls Ret-dependent and Ret-

independent events during development of nonpeptidergic DRG neurons. Neuron *54*, 739-754.

McDonagh, S. C., Lee, J., Izzo, A., and Brubaker, P. L. (2007). Role of glial cell-line derived neurotropic factor family receptor alpha2 in the actions of the glucagon-like peptides on the murine intestine. Am J Physiol Gastrointest Liver Physiol *293*, G461-468.

Moll, I., Paus, R., and Moll, R. (1996). Merkel cells in mouse skin: intermediate filament pattern, localization, and hair cycle-dependent density. J Invest Dermatol *106*, 281-286.

Moqrich, A., Earley, T. J., Watson, J., Andahazy, M., Backus, C., Martin-Zanca, D., Wright, D. E., Reichardt, L. F., and Patapoutian, A. (2004). Expressing TrkC from the TrkA locus causes a subset of dorsal root ganglia neurons to switch fate. Nat Neurosci *7*, 812-818.

Peters, E. M., Botchkarev, V. A., Muller-Rover, S., Moll, I., Rice, F. L., and Paus, R. (2002). Developmental timing of hair follicle and dorsal skin innervation in mice. J Comp Neurol *448*, 28-52.

Uesaka, T., Nagashimada, M., Yonemura, S., and Enomoto, H. (2008). Diminished Ret expression compromises neuronal survival in the colon and causes intestinal aganglionosis in mice. J Clin Invest *118*, 1890-1898.

Zylka, M. J., Rice, F. L., and Anderson, D. J. (2005). Topographically distinct epidermal nociceptive circuits revealed by axonal tracers targeted to Mrgprd. Neuron *45*, 17-25.